DEMONSTRATION OF SUB-1 HZ STRUCTURAL SYMMETRY IN MICRO-GLASSBLOWN WINEGLASS RESONATORS WITH INTEGRATED ELECTRODES

D. Senkal, M.J. Ahamed, A.A. Trusov, and A.M. Shkel
MicroSystems Laboratory, University of California, Irvine, CA, USA

ABSTRACT

We demonstrate, for the first time, sub-1 Hz frequency symmetry in micro-glassblown wineglass resonators with integrated electrode structures. A new fabrication process based on deep glass dry etching was developed to fabricate micro-wineglasses with self-aligned stem structures and integrated electrodes. The wineglass modes were identified by electrostatic excitation and mapping the velocity of motion along the perimeter using laser Doppler vibrometry. A frequency split (Δf) of 0.15 Hz and 0.2 Hz was observed for n = 2 and n=3 wineglass modes respectively. Frequency split stayed below 1 Hz for DC bias voltages up to 100 V, confirming that the low frequency split is attributed to high structural symmetry and not to capacitive tuning. High structural symmetry (<1 Hz) and atomically smooth surfaces (0.23 nm Sa) of the resonators may enable new classes of high performance 3-D MEMS devices, such as rate-integrating MEMS gyroscopes.

KEYWORDS

Micro-glassblowing, wineglass resonator, 3-D MEMS, degenerate wineglass modes, structural symmetry.

INTRODUCTION

Motivated by the proven performance of macro-scale Hemispherical Resonator Gyroscopes (HRG) [1], there has been a growing interest in 3-D MEMS wineglass resonator architectures for use in timing and inertial sensing applications. For example. devices such as rate integrating gyroscopes and mode-matched angular rate gyroscopes rely heavily on the stiffness (Δf) and damping ($\Delta \tau$) symmetry for high performance operation [2]. Wineglass architectures may enable MEMS-scale integration of these applications due to potential advantages in symmetry, minimization of energy losses and immunity to external vibrations [1].

However, wafer-scale fabrication of smooth, symmetric and high aspect ratio 3-D structures through micro-machining processes remains to be a challenge. This is mainly due to low relative tolerances and low aspect ratios (2.5-D) associated with conventional micro-machining processes. Factors such as mold non-uniformity, alignment errors or high surface roughness and granularity of deposited thin films have so far prevented the integration of 3-D wineglass structures with MEMS techniques. For example hemispherical shells were fabricated by thermally growing oxide in isotropically etched cavities, lowest as-fabricated frequency split was reported at 94 Hz [3]. Diamond hemispherical shells were also fabricated, using micro-crystalline diamond deposition into hemi-spherical molds, a frequency split of ~770 Hz was reported at ~35 kHz center frequency [4]. A similar process based on deposition of silicon nitride thin films and isotropic etching of silicon has also been explored by [5], minimum etch non-uniformity of 1.4 % was observed inside the molds due to the crystalline orientation dependent preferential etching in silicon. This effect may be a contributing factor in frequency asymmetry observed in [3] and [4]. Alternative fabrication techniques include thin film deposition onto high-precision ball bearings by [6] and blow-molding of bulk metallic glasses by [7] or blow-torch molding of fused silica by [8]. Q-factors as high ~300,000 were observed on blow-torch molded devices, however relative frequency splits ($\Delta f_{n=2}/f_{n=2}$) were on the order of 0.24~% to 4.49 % [8]. A ~2x variation in central frequency was also observed, which was associated with variations in molding duration and the consequent thickness variation.

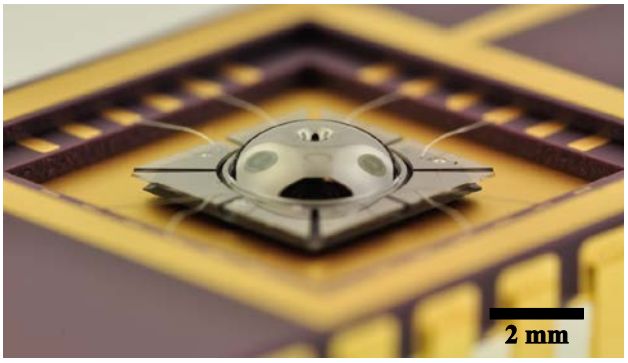

Figure 1: Metallized micro-wineglass structure with integrated electrodes. Diameter 4.4 mm, thickness 50 µm.

In this paper, we explore an alternative approach under the hypothesis that surface tension and pressure driven micro-glassblowing paradigm may serve as an enabling mechanism for wafer-scale fabrication of extremely symmetric ($\Delta f < 1$ Hz) and atomically smooth (0.23 nm Sa) 3-D wineglass structures. During micro-glassblowing, the 3-D shell structure undergoes viscous deformation due to the influence of surface tension and pressure forces [9-11]. The surface tension forces act on the 3-D shell structure at an atomic level to minimize surface roughness and structural imperfections, leading to atomically smooth surfaces and high structural symmetry. The micro-glassblowing process has also been demonstrated on low internal-loss materials such as Ultra Low Expansion Titania Silica Glass (ULE TSG) and fused silica at temperatures as high as 1700 °C [12,13], paving the way for ULE TSG and fused silica MEMS wineglass resonators. Characterization methods to identify wineglass modes were later presented in [14] by using assembled electrode structures and mechanical stimuli.

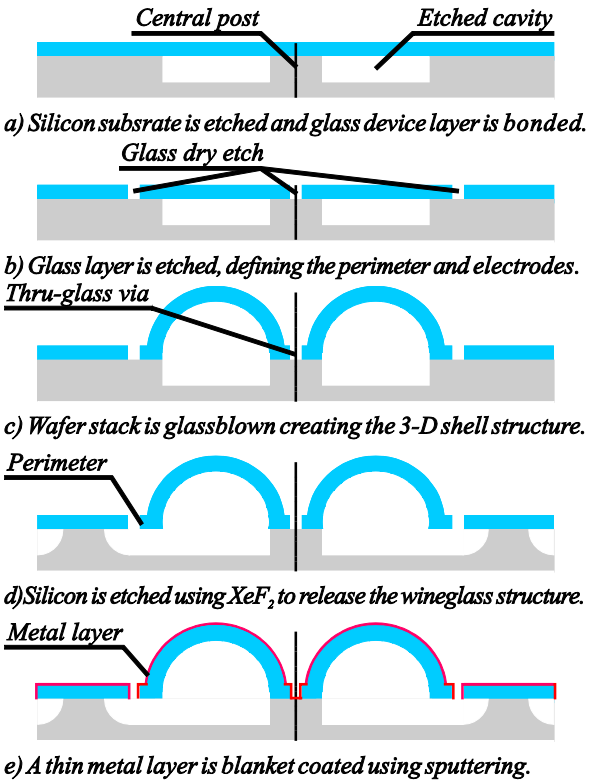

Figure 2: Process flow for fabricating micro-glassblown wineglass resonators with integrated electrodes.

In the following sections we will present improvements in fabrication process to incorporate in-situ electrode structures to the micro-glassblown resonators as well as further improvement in as-fabricated frequency split, demonstrating $\Delta f < 1$ Hz.

FABRICATION PROCESS

Fabrication process was optimized with two design goals in mind: (1) compatibility with batch-scale fabrication techniques, (2) elimination of process steps that can contribute to frequency asymmetry.

For compatibility with batch-scale fabrication techniques, standard micro-machining processes were used throughout the fabrication of the micro-wineglass resonators, such as lithography, dry etching, electroplating, sputtering etc. The glassblowing is performed in a standard rapid thermal annealing system, Heatpulse 610 RTA., which can provide uniform heating and cooling up to 6" diameter wafers.

In order to minimize the frequency asymmetry, several precautions were taken. This includes, elimination of pick-and-place or wafer alignment steps that can create misalignments and potentially contribute to frequency asymmetry. Also, contribution of mask misalignment errors were minimized by incorporating only two lithography steps and using a self-aligned stem structure. Both of the lithography steps are performed while the device is still in 2-D, eliminating the need for more challenging patterning techniques such as 3-D lithography, shadow masks or laser ablation of the 3-D structure. Finally, anisotropic dry etching was used to define both the substrate cavity and the outer perimeter of the structure, eliminating etch asymmetries that may occur due to crystalline orientation of silicon [5].

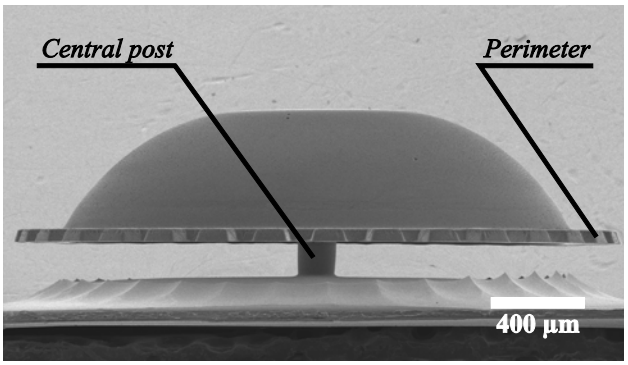

Figure 3: SEM image of a stand-alone micro-wineglass structure after release. Diameter 4.4 mm, thickness 50 µm.

In order to fabricate the micro-wineglass resonators, first cylindrical cavities with a central post are etched to a at 250 µm depth on a silicon substrate wafer using DRIE, Fig. 2(a). Then a thin glass layer (100 µm) is anodically bonded onto the silicon substrate. The glass layer bonds to the substrate along the perimeter of the cylindrical cavity and at the central post. This is followed by deep glass dry etching of the outer perimeter of the wineglass resonator and central via hole Fig. 2(b). Capacitive gaps and individual electrodes are also defined at this step. The glass etching is performed using a magnetic neutral loop discharge plasma oxide etcher (ULVAC NLD 570 Oxide Etcher). A ~5 µm thick low-stress electroplated Cr/Ni hard-mask was used to etch the 100 µm deep trenches. This is followed by micro-glassblowing of the wafer stack at 875 °C inside a RTA system, where the glass layer becomes viscous and the air inside the cavity expands, creating the 3-D shell structure, Fig. 2(c). The perimeter of the wineglass structure and the planar electrodes do not deform as there is no etched cavity under these structures, enabling lithographic definition of the capacitive gaps. The next step is XeF_2 etching of the substrate underneath the glass layer in order to release the wineglass resonator along its perimeter, Fig. 2(d). XeF_2 is chosen because of the extremely high selectivity to glass (as high as 1:1000 selectivity). Once the etch is complete a free standing micro-wineglass structure with a self-alinged stem structure is obtained, Fig 3.

Final step of the fabrication process is blanket metallization by sputtering, Fig. 2(e). A monolayer of Iridium is chosen for the metal layer, because of high conductivity, corrosion resistance and the ability to apply without utilizing an adhesion layer. The metal layer coats the top surface of the resonator shell, the side walls of the capacitive gaps as well as inside of the central via hole. However, directionality of the sputtering process prevents the metal layer from coating the undercut created by the XeF_2 etch, electrically isolating the electrodes and the resonator. Electrical feed-through to the resonator is obtained through the central via structure, which connects the resonator onto the substrate.

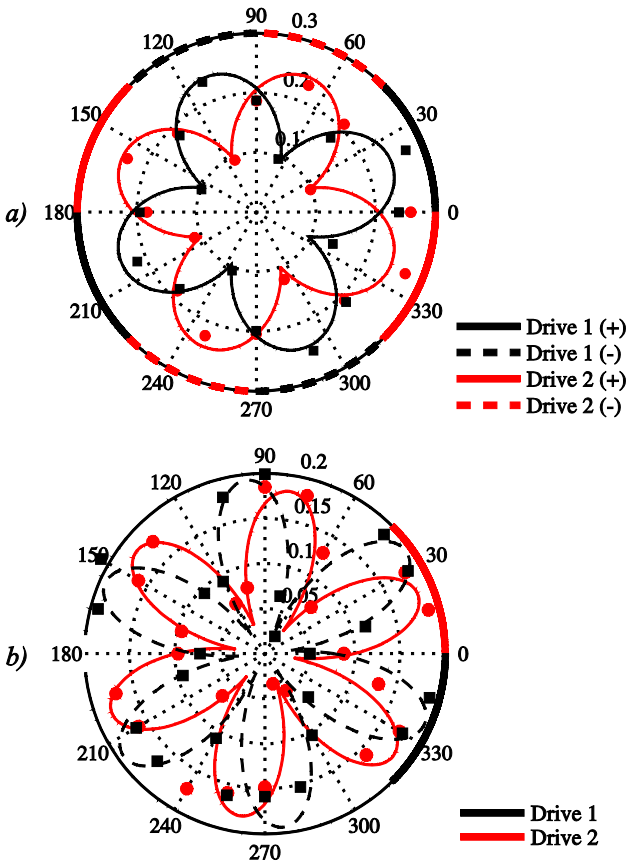

Figure 4: Measured velocity amplitude distribution (mm/s) identifying (a) n=2 and (b) n=3 wineglass modes.

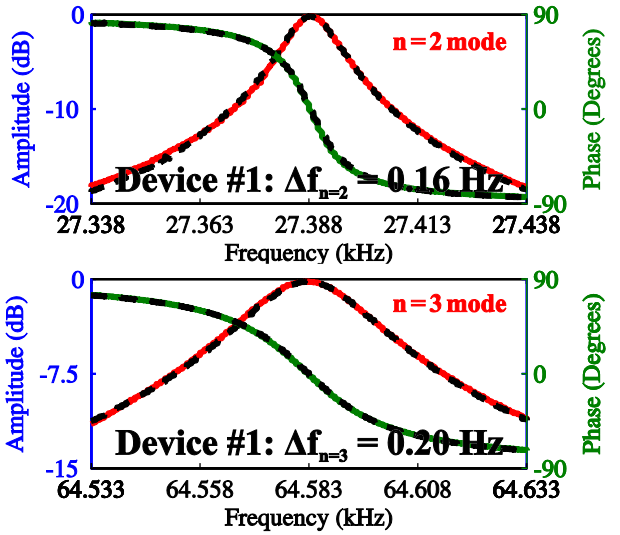

Figure 5: Frequency sweeps of n=2 and n=3 wineglass modes, showing Δf = 0.16 Hz and Δf = 0.20 Hz respectively.

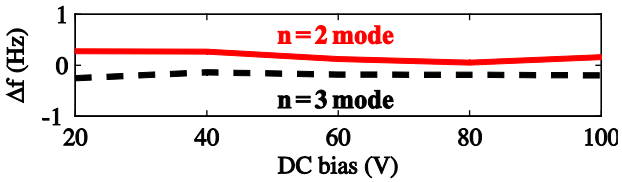

Figure 6: Frequency split vs DC bias, showing that the frequency split is within 0.2 Hz independent of DC bias.

TESTING & CHARACTERIZATION

In order to identify the mode shapes associated with different resonant frequencies, the wineglass resonator was excited electrostatically using the integrated electrode structures. The amplitude of motion at different points along the outer perimeter was mapped using laser Doppler vibrometry, creating a representation of the mode-shapes associated with different resonant frequencies. This was accomplished by moving the laser spot along the perimeter while driving the resonator with two different sets of electrode configurations for each degenerate wineglass mode. For n = 2 wineglass mode, 4 electrodes were used for each degenerate mode with 45° angle between the two electrode sets. Two of the electrodes were driven in anti-phase, this kind of electrode configuration excites the n = 2 wineglass mode selectively, while suppressing all other modes. For n = 3 mode a single electrode was used for each degenerate wineglass mode, as a balanced excitation using 2 or 4 electrodes inherently suppresses the n = 3 mode. A DC bias voltage of 100 V and an AC drive voltage of 5 V was used in all experiments (V_{DC} = 100 V and V_{AC} = 5 V).

For device #1, center frequencies of degenerate wineglass modes were identified at 27389 Hz and 64583 Hz for n = 2 and n = 3 wineglass modes respectively, Fig. 4. Frequency split between the two degenerate modes were measured by fitting a second order system response onto the frequency sweep data of each degenerate wineglass mode. A frequency split (Δf) of 0.16 Hz and 0.2 Hz was observed for n=2 and n=3 wineglass modes respectively with 95% confidence levels at 0.23 Hz for n = 2 and 0.3 Hz for n = 3, Fig. 5. In order to estimate the contribution of electrostatic spring softening effect, DC bias voltage was varied between 20 V - 100 V, frequency split stayed below 1 Hz for both modes, attributing the low frequency split to high structural symmetry and not to capacitive tuning, Fig. 6.

In order to verify the repeatability of the results, four other wineglass resonators from the same wafer were characterized using the method described above. Three of the five wineglass resonators had frequency split less than 5 Hz for the n = 2 wineglass mode, with one outlier at Δf ≈ ~21 Hz, Fig. 7 and Table 1.

CONCLUSIONS

Micro-glassblown resonators with integrated electrode structures were fabricated. Electrostatic excitation of micro-glassblown resonators using integrated electrode structures were experimentally demonstrated for the first time. Identification of the mode shapes using laser Doppler vibrometry revealed frequency splits as low as $\Delta f_{n=} < 1$ Hz at ~27 kHz center frequency, giving a relative frequency split of $\Delta f_{n=2}/f_{n=2} < 10$ ppm, Table 1. These results demonstrate the feasibility of surface tension driven micro-glassblowing process as a means to fabricate extremely symmetric and smooth 3-D wineglass resonators.

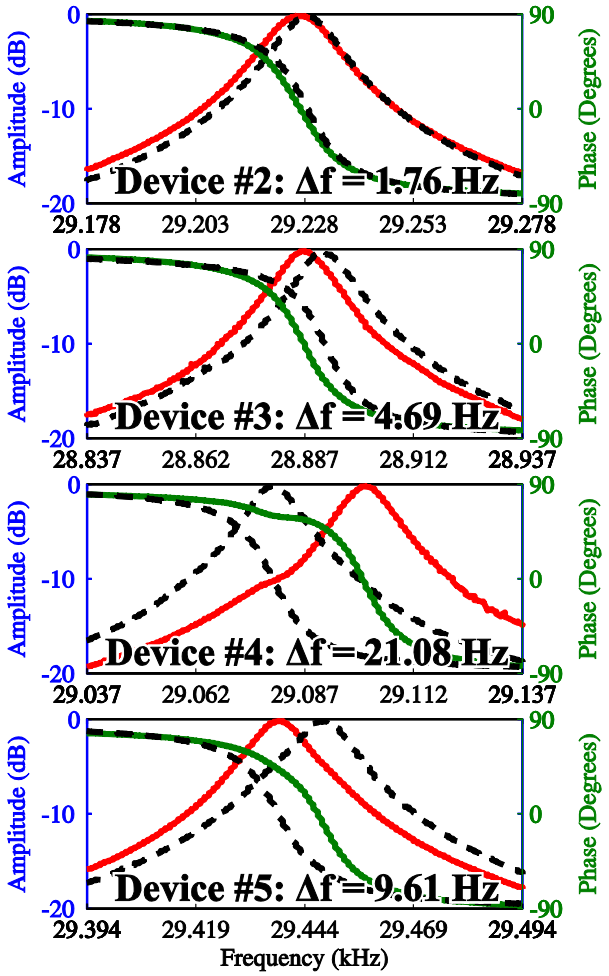

Figure 7: Frequency sweeps of n = 2 *mode of 4 additional wineglass resonators, showing* Δf *values in the range of 1.76 Hz to 21.08 Hz.*

Table 1: Summary of as-fabricated frequency split on 5 micro-glassblown wineglass resonators.

Device #	Center Freq.	Δf (Hz)	σ (Hz)	Δf/f (ppm)
1	27388.65	0.16	0.04	5.67
2	28889.18	4.69	0.05	162.18
3	29227.60	1.76	0.05	60.30
4	29090.38	21.08	0.06	724.65
5	29442.98	9.61	0.07	326.40

High structural symmetry (Δf <1 Hz) and atomically smooth surfaces (0.23 nm Sa) of the resonators may enable new classes of high performance 3-D MEMS devices, such as rate-integrating MEMS gyroscopes and mode-matched angular rate gyroscopes.

ACKNOWLEDGEMENTS

This material is based upon work supported by DARPA grant W31P4Q-11-1-0006 (Program Manager Dr. William Chappell). Devices were designed and tested in UCI MicroSystems Lab. Authors would like to thank UCI INRF staff Jake Hes, Mo Kebaili, Vu Phan and Lifeng Zheng for their help and valuable suggestions on the fabrication aspects of the project.

REFERENCES

[1] D.M. Rozelle, "The hemispherical resonator gyro: From wineglass to the planets", in *Proc. AAS/AIAA Space Flight Mechanic*, Feb. 2009, pp. 1157–1178.

[2] C. Painter and A. Shkel, "Active structural error suppression in MEMS vibratory rate integrating gyroscopes," *Sensors Journal, IEEE*, vol. 3, no. 5, pp. 595–606, 2003.

[3] L.D. Sorenson, P. Shao, F. Ayazi, and C. Engineering, "Effect of thickness anisotropy on degenerate modes in oxide micro-hemispherical shell resonators," in *IEEE MEMS 2013*, no. 111.

[4] M.L. Chan, J. Xie, P. Fonda, H. Najar, K. Yamazaki, L. Lin, and D. A. Horsley, "Micromachined polycrystalline diamond hemispherical shell resonators," in *Technologies for Future Micro-Nano Manufacturing Workshop 2011*, 2012, pp. 355–358.

[5] C.L. Fegely, D.N. Hutchison, S.A. Bhave, "Isotropic etching of 111 SCS for wafer-scale manufacturing of perfectly hemispherical silicon molds," *Proc. Transducers'11*, Beijing, China, June 5-9, pp 2595-2598.

[6] Y. Xie, H.C. Hsieh, P. Pai, H. Kim, M. Tabib-Azar, and C. H. Mastrangelo, "Precision curved micro hemispherical resonator shells fabricated by poached-egg micro-molding," in IEEE Sensors 2012, 2012, pp. 1–4.

[7] B. Sarac, G. Kumar, T. Hodges, S. Ding, A. Desai, J. Schroers, "Three-Dimensional shell fabrication using blow molding of bulk metallic glass," *IEEE J. Microelectromech. Syst.*, vol. 20, no. 1, pp. 28-36, 2011.

[8] J. Cho, J. Yan, J. Gregory, and H. Eberhart, "High-q fused silica birdbath and hemispherical 3-D resonators made by blow torch molding," in *IEEE MEMS 2013 Conference*, 2013, pp. 177–180.

[9] E.J. Eklund and A.M. Shkel, "Method and apparatus for wafer-level micro-glass-blowing," US Patent 7694531, Issued April 13, 2010.

[10] I.P Prikhodko, S.A. Zotov, A.A. Trusov A.M. Shkel, "Microscale glass-blown three-dimensional spherical shell resonators," *IEEE J. Microelectromech. Syst.*, vol. 20, no. 3, pp.691-701, 2011.

[11] S.A. Zotov, I.P. Prikhodko, A. A. Trusov, and A. M. Shkel, "3-D micromachined spherical shell resonators with integrated electromagnetic and electrostatic transducers," in *Solid-State Sensors, Actuators, and Microsystems Workshop 2010*, pp. 11–14.

[12] D. Senkal, C. Raum, A.A. Trusov, and A.M. Shkel, "Titania silicate/fused quartz glassblowing for 3-D fabrication of low internal loss wineglass micro-structures," in *Solid-State Sensors, Actuators, and Microsystems Workshop 2012*, 2012, pp. 267–270.

[13] D. Senkal, M.J. Ahamed, A.A. Trusov, and A.M. Shkel, "High temperature micro-glassblowing process demonstrated on fused quartz and ULE TSG," in *Sensors and Actuators A: Physical*, (In print).

[14] D. Senkal, M.J. Ahamed, A.A. Trusov, and A.M. Shkel, "Adaptable test-bed for characterization of micro-wineglass resonators," in *IEEE MEMS '13*, pp. 469–472.

CONTACT

D. Senkal, tel: +1-949-689-3370; dsenkal@uci.edu.